A Multireference Configuration Interaction Investigation of the Excited-State Energy Surfaces of Fluoroethylene (C_2H_3F)

Mario Barbatti,* Adélia J. A. Aquino, and Hans Lischka†

Institute for Theoretical Chemistry, University of Vienna, Währingerstrasse 17, A-1090 Vienna, Austria

Received: February 17, 2005; In Final Form: April 22, 2005

Multireference configuration interaction with singles and doubles (MR-CISD) calculations has been performed for the optimization of conical intersections and stationary points on the fluoroethylene excited-state energy surfaces. For the planar ground state geometry, the vertical spectrum including 3s and 3p Rydberg states was calculated. From this geometry, a rigid torsion around the CC bond strongly reduces the energy gap between S_0 and S_1 states. Furthermore, a search for the minimum of the crossing seam shows that there exists a conical intersection close to the twisted structure and two additional ones for cis and trans pyramidalized structures. These three intersections are connected by the same seam. We have shown that the Hula-Twist process is an alternative way to the direct CC twisting in order to reach this part of the seam. Other conical intersections were also located in the CH_3CF and CH_2FCH, H-migration, and C_{3v} structures. The photodynamics of the system is discussed based on topological features of these intersections.

1. Introduction

It is well-known that conical intersections act as funnels allowing fast, radiationless transfer to another electronic state. Actually, these intersections span a $(N-2)$-dimensional space, the intersection seam.[1,2] The properties of the conical intersections make the crossing seam the very heart of the ultrafast photodynamical processes and a great effort has been devoted to its characterization, mainly of its minima. Despite the significant progress achieved in the last years in the development of methods[2−5] and in the study of the conical intersections for even relatively large molecules,[6−9] several questions still arise, such as those concerning the extension of the seam and the role that each part is playing during the dynamics. Attempts to answer this kind of question have been recently performed by using ethylene as a prototype molecule.[10,11] The break of symmetry introduced by substituted ethylenes, such as $H_2C=XH_2$ or $C_2H_nX_{4-n}$, can furnish valuable information about the electronic structures involved in the crossing seam. Recently, silaethylene $(CSiH_4)$[12] and the methyleneimmonium cation $(CNH_4{}^+)$[13] have been studied in our group. The haloethylenes $C_2H_nX_{4-n}$ (X = F, Cl, Br), and in particular fluorethylene (X = F, n = 3)—the subject of the present work—comprise examples of a different kind since the polarity of the π bond is achieved by a link to the C=C bond and not by substitution of a carbon atom.

An important topic in the research of haloethylenes is the determination of the elementary processes resulting in the molecular fragmentation, such as the hydrogen halide and molecular hydrogen eliminations.[14−17] These eliminations can involve the H and the halide atoms attached to the same C atom (three-center $\alpha\alpha$-elimination) or atoms on different C atoms (four-center $\alpha\beta$-elimination). Since the work of Berry and Pimentel,[14] which presented the first experimental results for the HF elimination after a photoexcitation, numerous theoretical

and experimental investigations have been dedicated to this subject,[14,23] especially in treating the ground-state structures and processes. Kato and Morokuma[15] showed that in the case of fluoroethylene the simple determination of the reaction path was not sufficient to decide between the three- and four-center HF elimination. On the basis of the HF translational energy release after 157 nm $(\pi\pi^*)$ photoexcitation, Sato and co-workers[23] concluded that the four-center $\alpha\beta$-elimination should be the dominant process. However, the HX (X = F, Cl, Br) rovibrational distribution obtained from the photolysis of CH_3X at 193 nm[16,17] has shown that the three-center process is the dominant one.

Besides HF elimination, Kato and Morokuma[15] investigated several reaction channels on the ground and first triplet energy surfaces of fluoroethylene including H-migration and cis−trans isomerization. Smith, Coffey, and Radom[24] systematically studied the ground-state equilibrium geometry at several ab initio levels. Martínez-Núñez and Vásquez[25] investigated the fragmentation reactions in the ground state. Recently, they have furnished theoretical results about the rovibrational distribution of the HF fragments in the photodissociation process.[22] Also recently, Ljubić and Sabljić[26] and Lie and co-workers[27] have investigated the reaction mechanisms of fluoroethylene and ozone. Kunsági-Máté et al.[21] have employed AM1 semiempirical molecular dynamics to investigate the influence of the environment on the HF elimination. To the best of our knowledge, Bacskay[28] was the only one to perform ab initio calculations on the first singlet-excited state of fluoroethylene investigating the isomerization and fragmentation processes.

In the present work, our main goal is to characterize the lowest excited-state energy surfaces of fluoroethylene with particular emphasis on the crossing seam between the S_0 and S_1 states, and to discuss the role that it has in the photochemistry of this system. Although our research is not primarily concerned with the fragmentation topic, we believe that the characterization of the first singlet excited state and of the S_0/S_1 crossing seam can furnish new and valuable information about this process.

* Address correspondence to this author. E-mail: mario.barbatti@univie.ac.at.
† E-mail: hans.lischka@univie.ac.at.

Excited-State Energy Surfaces of Fluoroethylene

J. Phys. Chem. A, Vol. 109, No. 23, 2005 **5169**

We also present ab initio results for the vertical spectrum of fluoroethylene, including in total six valence and Rydberg singlet-excited states.

2. Computational Details

State-averaged multiconfiguration self-consistent field (SA-MCSCF) and multireference configuration interaction with singles and doubles (MR-CISD) calculations were carried out. In the SA-MCSCF calculations equal weights were used for all states. Two different active spaces were chosen in the MCSCF calculations. For the description of valence states, the wave function was a CAS(2,2) in the π and π^* orbitals. State averaging was performed over the states N (π^2), V ($\pi\pi^*$), and Z (π^{*2}). The same CAS(2,2) was used as reference space in the subsequent MR-CISD calculations. The final expansion space for the MR-CISD calculations in terms of configuration state functions (CSFs) consisted of the reference configurations and of all single and double excitations thereof into all internal and external orbitals. The interacting space restriction[29] was applied. The three core orbitals were always kept frozen in the post-MCSCF calculations. Analogous principles for the construction of the CI wave function were applied for the larger reference space used in the calculation of the Rydberg states described below. The MR-CISD/CAS(2,2) calculations were used for the determination of the minima on the crossing seam (MXS), for the calculation of stationary points, and for the cuts of the potential energy surface. In general, all optimizations were performed without symmetry restrictions. The aug-cc-pVDZ basis[30,31] was selected in these calculations. All stationary points and MXSs were reoptimized with an aug'-cc-VTZ basis set, which was derived from the original aug-cc-pVTZ set by omitting the augmented f functions on the carbon atoms and all d functions on the hydrogen atoms. Size-extensivity corrections were taken into account by means of the extended Davidson correction[32,33] and will be denoted by +Q.

For the joint calculation of valence and Rydberg states, the $\pi\pi^*$-CAS(2,2) was augmented by four auxiliary (AUX) orbitals representing the 3s and 3p Rydberg orbitals. Only single excitations were allowed from the CAS to the AUX space. In addition to the three valence states N, V, and Z, four Rydberg states (π–3s, π–$3p_x$, π–$3p_y$, and π–$3p_z$) were considered leading to a state-averaging over seven states at the MCSCF level. The same configuration space was used as reference space in the MR-CISD calculations and is denoted as MR-CISD/SA-7-CAS(2,2)+AUX(4). A d'-aug-cc-pVDZ basis[30,31,34,35] was chosen to take into account the diffuseness of the Rydberg orbitals. On this basis, d' stands for the original d-augmented set of diffuse basis functions but omitting the doubly augmented d functions on the carbon atoms and the doubly augmented p function on the hydrogen atoms.

Although the calculations at the MR-CISD/SA-7-CAS-(2,2)+AUX(4)/d'-aug-cc-pVDZ level produce satisfactory results in torsional angles larger than 20°, for the planar and quasiplanar geometries the treatment at this level is not sufficient. The π–$3p_x$ state is located below the $\pi\pi^*$ state, in contradiction to the experimental results (see Subsection 3a). This effect occurs due to a strong mixing between the π and $3p_x$ molecular orbitals, which also appears in other systems such as ethylene[36] and butadiene.[37]

To obtain a more adequate description of the vertical excitations, the aforementioned CAS(2,2)+AUX(4) reference space was augmented by a restricted direct product (RDP) space[38] constructed for all σ orbitals. The RDP space is composed of 14 orbitals grouped in seven subspaces, one for each σ bond and the lone pair, i.e., three $[\sigma-\sigma^*]_{CH}$, one $[\sigma-\sigma^*]_{CC}$, one $[\sigma-\sigma^*]_{CF}$, and two $[\sigma-\sigma^*]_{n(F)}$ pairs. Each $\sigma-\sigma^*$ subspace is restricted to singlet pairing. The MCSCF calculation based on the RDP wave function resulted in localized orbitals very similar to those obtained in generalized valence bond (GVB) calculations.[39] The molecular orbitals obtained in this RDP(σ)+CAS(2,2)+AUX(4) space were used for the subsequent MR-CISD calculation. The reference space was composed of all previously used CAS(2,2)+AUX(4) configurations plus all single excitations from the σ_{CC} and σ_{CF} orbitals to the CAS, AUX, σ_{CC}^*, and σ_{CF}^* orbitals. The remaining σ orbitals were transferred to the reference doubly occupied space and the corresponding σ^* orbitals to the virtual space. We denote this level as MR-CISD/SA-7-[RDP+CAS(2,2)+AUX(4)].

Although the π^* and $3p_x$ orbitals resulting from the MCSCF calculation in this improved RDP space are still strongly mixed, the introduction of the $\sigma-\pi$ correlation at the reference level and of concomitant higher excitations at the MR-CISD have a significant effect on the final result by stabilizing the V state and reducing the mixing with the π–$3p_x$ state.

The ground-state geometry and the vertical spectrum were calculated also by means of the resolution of the identity approximate coupled cluster singles and doubles (RI-CC2) method.[40–43] For the geometry optimization of the ground state the aug'-cc-pVTZ basis set was used. The vertical excitation spectrum was obtained with the d'-aug-cc-pVDZ basis set.

For the geometry optimizations, analytic MR-CISD energy gradients were computed by using the procedures described in refs 44–47. Determinations of the minima on the crossing seam (MXS) were performed by using the analytic MR-CI nonadiabatic coupling vectors[4] and the direct inversion in the interactive subspace (GDIIS) procedure developed in ref 48. Standard GDIIS optimization[49] was used for the determination of stationary points. Natural internal coordinates were constructed according to the directions given in ref 50.

Optimized geometries, energies, and conical intersections were obtained with the COLUMBUS program system.[51–54] The atomic orbital (AO) integrals and AO gradient integrals have been computed with program modules taken from DALTON.[55] The RI-CC2 calculations were performed with the TURBOMOLE program package.[56]

3. Results and Discussions

3.a. Vertical Excitations, CC Torsion, and Rydberg States. The ground-state equilibrium geometry of the C_2H_3F system is planar and belongs to the C_s point group (Figure 1). The computed geometries are in good agreement with the experimental ones[24] (see Table 1). The effect of improving the basis set from the double to the triple-ζ level is to get an overall reduction of the CC and CH bond distances by about 0.01 Å (0.02 Å in the case of the CF bond distance). The same pattern of bond-distance shortening is also observed in the optimization of all other stationary structures and conical intersections that will be discussed in Subsections 3.c and 3.d.

The absorption spectra of several haloethylenes were measured by Bélanger and Sadorfy.[57] The spectrum of the C_2H_3F species shows a broad peak for the V-state ($\pi\pi^*$) centered at 7.44 eV, superimposed by several sharp peaks assigned to Rydberg transitions. Different from ethylene, the fluoroethylene absorption spectrum does not present a long low-energy progression. The π–3s transition was assigned to the 6.89 eV peak. The 8.09 eV peak was assigned as the π–$3p_x$ transition.

Except for the π–$3p_x$ and π–π^* transitions, the RI-CC2 and MR-CISD methods present quite similar transition energies (see
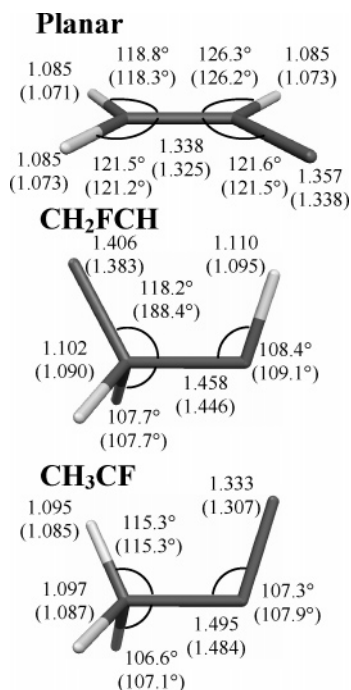
Planar

Figure 1. Structures and selected parameters of the stationary structures optimized at the L1 (L2) level defined in Table 3. Distances in Å and angles in deg.

TABLE 1: Selected Geometric Parameters[a] for the Planar Ground State Minimum

	L1[b]	L2[c]	CC2[d]	exptl[e]
C_1C_2	1.338	1.325	1.327	1.329
C_1F	1.357	1.338	1.358	1.346
C_1H	1.085	1.073	1.090	1.077
C_2H_C	1.085	1.071	1.088	1.081
C_2H_T	1.085	1.073	1.089	1.081
C_2C_1F	121.6	121.5	122.0	121.5
C_2C_1H	126.3	126.2	126.4	125.4
$C_1C_2H_C$	118.8	119.3	118.9	118.6
$C_1C_2H_T$	121.5	121.2	121.9	120.9

[a] Distances in Å and angles in degrees. [b] L1 = MR-CISD/SA-3-CAS(2,2)/aug-cc-pVDZ. [c] L2 = MR-CISD/SA-3-CAS(2,2)/aug′-cc-pVTZ. [d] RI-CC2/aug′-cc-pVTZ. [e] Reference 24.

Table 2) with good agreement for the experimental $\pi-3s$ transition. The addition of the Davidson corrections (+Q) to the MR-CISD results produces a systematic increase of the Rydberg excitation energies by about 0.3 eV. Our best MR-CISD+Q result for the vertical $\pi-\pi^*$ transition is still 0.4 eV above the experimental result. This shows that similar difficulties with the description of this state occur as in ethylene (see ref 36 and references therein). Also the RI-CC2 calculations give only a slightly better value. To resolve this discrepancy significantly more extended calculations would have to be performed and possible effects of the vibrational structure and nonadiabatic couplings similar to ethylene[58] need to be considered. Moreover, we note that the experimentally observed band is very broad and the determination of the band maximum seems to be somewhat arbitrary. Since our aim is the investigation of energy surfaces and conical intersections far away from the region of the vertical excitation, we did not pursue this question further.

The values for the oscillator strength show that, as expected, the optical absorption is dominated by the V state, but with some contributions from the $\pi-3p_x$ and $\pi-3s$ states. The high-energy π^{*2} state (Z) is shown in Table 2 just because it can be obtained also within the $\pi\pi^*$-CAS(2,2) space. However, we

should bear in mind that between the V and the Z states a multitude of other states will be located, including those involving the $\sigma^*(C-F)$ orbital.

As is shown in Figure 2, the Rydberg states are destabilized by the torsional coordinate, while the V and Z states decrease in energy and ultimately become the lowest excited states. A similar behavior was found in the case of ethylene.[58,59] This means that the cis−trans isomerization can occur without barrier in the V or Z states. The V state crosses all Rydberg states for torsional angles between 0° and 30°, and after that it becomes the S_1 state. Due to its high energy in the planar geometry, the Z state crosses the Rydberg states in the region from 60° to 75°. Finally, it becomes the S_2 state.

For ethylene, the Z state crosses the V state at a torsional angle of 86°[10,60] and these two states are almost degenerate at 90°. In the present case, the stabilization of the Z state is not strong enough to allow this crossing and this state lies close to the Rydberg 3s state for the 90° twisted geometry, about 3.4 eV above the V state. For a rigid torsion one finds only a relatively small gap of 0.86 eV between the S_0 and S_1 states at 90°. If we optimize the twisted structure of the V state, this gap is reduced to 0.62 eV (see Table 3). As we will show below, these rather small gaps are a good indication that there is a crossing between the ground and V states near the twisted structure in contrast to the situation found for ethylene.

The qualitative difference in the torsional potential energy curves for ethylene and fluoroethylene can be rationalized by the 3×3 CI analytical model for biradicaloids developed by Bonačić-Koutecký et al.[61,62] This model predicts that for the type of nonsymmetric biradicaloids as is the case for fluoro-ethylene the S_1 state can become degenerate with S_0 by increasing the electronegativity difference of the CC bond. The just-described results for ethylene and fluoroethylene fit very well into this model.

3.b. Description of Isomers. Besides the planar global minimum CH_2CHF, we have characterized two other isomers of fluoroethylene on the S_0 surface, one with the structure CH_3-CF and another with the structure CH_2FCH. The structure and selected geometrical parameters of these isomers are shown in Figure 1. The energy of each structure is given in Table 3. The theoretical characterization of these two isomers at the SCF/4-31G level was carried out many years ago by Kato and Morokuma[15] and recently by Bacskay[28] for CH_3CF at the DFT and MR-CISD levels.

The isomer with the nonsubstituted CH_3 group is more stable than that with the CH_2F group, lying 2.32 eV (Table 3, L2Q level) above the ground-state global minimum. The isomer with the CH_2F group, on its turn, has its ground state 3.30 eV above the global minimum. Although we observe these strong differences in the ground state energies, the first-excited-state energies of the two isomers are practically the same, as we can see from Table 3.

Our result for the vertical S_0-S_1 excitation energy of the CH_3-CF isomer is 2.91 eV (Table 3, L2Q level), which is in good agreement with the 2.99 eV obtained by Bacskay at the MR-CISD+Q/cc-pVTZ level, but with geometry optimization at the B3LYP/cc-pVTZ level.

3.c. Minima on the Crossing Seam. As we discussed above, the small S_0/S_1 gap for the 90° twisted structure is an indication that there should be a crossing near it. Indeed, we succeeded in locating an intersection in a twisted structure with a slight character of hydrogen migration. Its geometrical parameters and energy are shown in Figure 3 and Table 4, respectively. Figure 4a shows the gradient difference vector $\mathbf{g}^{01}$ and the nonadiabatic

Excited-State Energy Surfaces of Fluoroethylene

J. Phys. Chem. A, Vol. 109, No. 23, 2005 **5171**

TABLE 2: C₂H₃F Vertical Excitations from the Planar Ground State Structure

state		MCSCF	MR-CISD	MR-CISD+Q[a]	CC2[b]	exptl[c]	oscillator strength[a]
N	$1^1A'$	0.00^d	0.00^e	0.00^f	0.00^g		
$\pi-3s$	$1^1A''$	5.89	7.15	7.42	7.12	6.98	0.06
$\pi-3p_{yz}$	$2^1A'$	6.49	7.78	8.06	7.74		0.00
$\pi-3p_{yz}$	$3^1A'$	6.72	7.98	8.26	7.99		0.00
V	$2^1A''$	8.33	7.86	7.86	7.72	7.44^h	0.29
$\pi-3p_x$	$3^1A''$	6.82	8.17	8.37	8.51	8.09	0.10
Z	n^1A'	14.09	13.51	13.05			0.00

ᵃ MR-CISD+Q/SA-7-[RDP+CAS(2,2)+AUX(4)]/d′-aug-cc-pVDZ. ᵇ RI-CC2/d′-aug-cc-pVDZ. ᶜ Reference 57. ᵈ $E = -176.988334$ au. ᵉ $E = -177.365055$ au. ᶠ $E = -177.422771$ au. ᵍ $E = -177.550517$ au. ʰ Maximum of the absorption band.

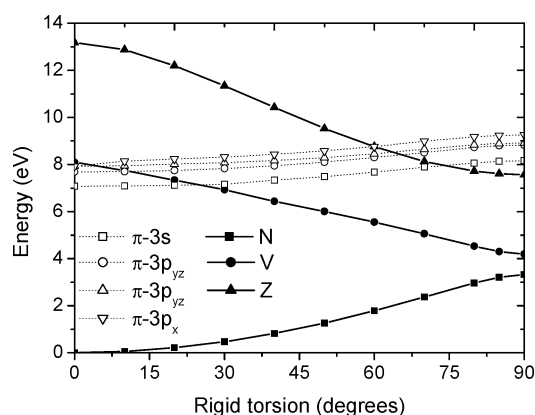**Figure 2.** Potential energy curves for the rigid torsion. The curves are plotted in a diabatic way following the character of the wave function.

TABLE 3: Ground- and Excited-State Energies of the Stationary Structures Optimized for the State S_k ($k = 0, 1$)[a]

			energy (eV)			
structure	k	state	L1	L1Q	L2	L2Q
planar	0	S_0	0.00^b	0.00^c	0.00^d	0.00^e
		S_1	8.24	7.94	8.29	7.99
twisted	0	S_0	3.11	2.98	3.24	3.13
		S_1	4.68	4.36	4.72	4.43
twisted	1	S_0	3.51	3.41	3.63	3.55
		S_1	4.27	4.03	4.31	4.10
CH₃CF	0	S_0	2.26	2.25	2.31	2.32
		S_1	5.19	5.18	5.23	5.23
CH₂FCH	0	S_0	3.14	3.18	3.25	3.30
		S_1	5.27	5.32	5.35	5.40

ᵃ The reference energy level is the planar ground state. ᵇ $E = -177.362514$ au. L1 = MR-CISD/SA-3-CAS(2,2)/aug-cc-pVDZ. ᶜ $E = -177.413880$ au. L1Q = MR-CISD+Q/SA-3-CAS(2,2)/aug-cc-pVDZ. ᵈ $E = -177.490127$ au. L2 = MR-CISD/SA-3-CAS(2,2)/aug′-cc-pVTZ. ᵉ $E = -177.549453$ au. L2Q = MR-CISD+Q/SA-3-CAS(2,2)/aug′-cc-pVTZ.

coupling vector $\mathbf{h}^{01}$. The g−h space is composed mainly of CC stretching, H-migration, and CC torsion. This situation is similar to that for the CSiH₄[12] and CNH₄[+13] molecules, for which the simple torsion also ends in an intersection.

For the twisted-orthogonal structure of ethylene there is a large S₀/S₁ gap of 2.35 eV.[59] To reach the conical intersection requires strong pyramidalization and partial hydrogen migration. For fluoroethylene the twisted structure is already an intersection and, furthermore, the seam continues along the pyramidalization of the CH₂ group and reaches one of the two MXS at angles of 122.4° (cis pyramidalized) and 122.9° (trans pyramidalized). The two MXS are characterized in Figure 3 and Table 4. In Figure 5 the path connecting the twisted intersection with the cis- and trans-pyramidalized MXS is shown in terms of the pyramidalization angle β. The geometries used to calculate this
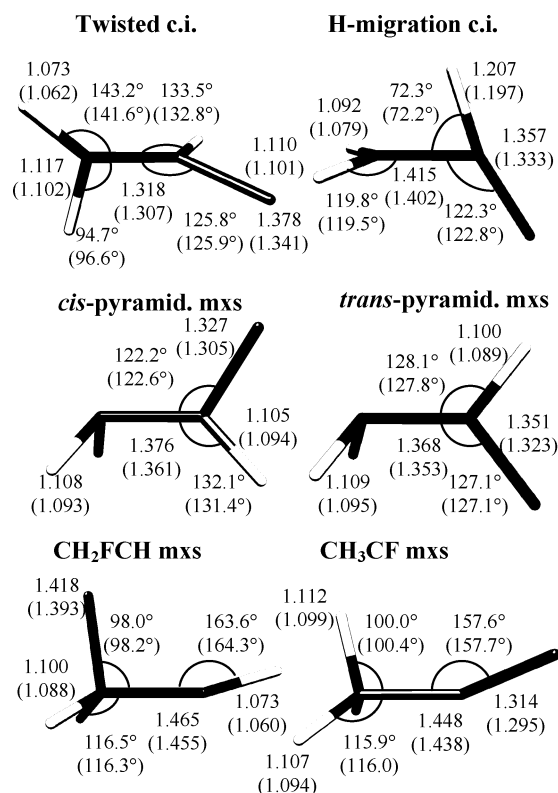

Figure 3. Geometrical structures and selected parameters for the conical intersections optimized at the L1 (L2) level defined in Table 3. The pyramidalization angles of the cis and trans pyramidalized MXSs are 119.2° (122.4°) and 120.4° (122.9°), respectively. Distances in Å and angles in deg.

TABLE 4: Energies of the S_0/S_1 Conical Intersections[a]

	energy (eV)			
structure[b]	L1	L1Q	L2	L2Q
cis pyramidal	4.10	3.92	4.15	3.91
trans pyramidal	4.12	3.96	4.19	3.94
twisted ci	4.39	4.28	4.42	4.21
CH₂FCH MXS	4.83	4.92	4.91	5.00
CH₃CF MXS	5.47	5.50	5.48	5.50
CH₃CF C_{3v}[c]	5.82	5.88	5.82	5.86
H-migration	6.38	6.11	6.48	6.24

ᵃ The zero energy level is the planar ground state (see Table 3). The computational levels (L) are defined in Table 3. ᵇ ci = conical intersection. MXS = minima on the crossing seam. ᶜ Geometry optimized at the S₁ state restricted to the C_{3v} point group.

path were obtained by a simple geometrical linear interpolation between the twisted conical intersection and each of the pyramidalized MXSs. Very flat curves are obtained. Figure 5 shows that already this procedure leads to a path very close to the seam. Therefore, we did not consider it necessary to optimize this path completely. An analogous path on the seam exists in
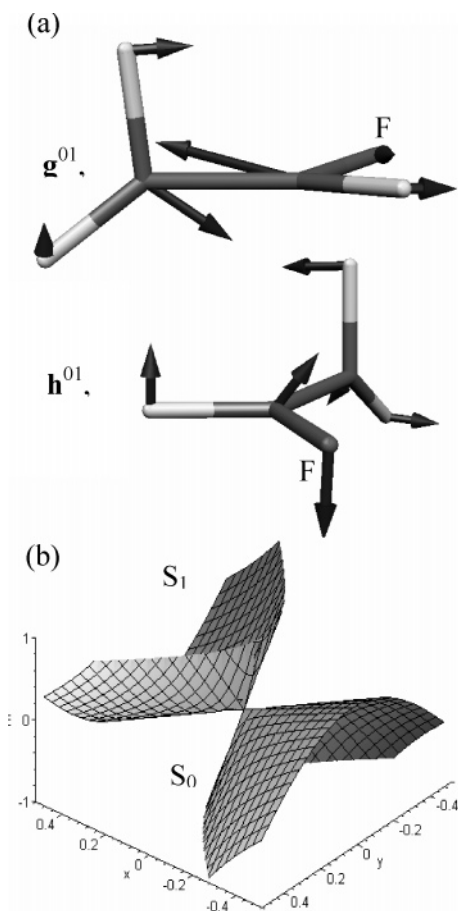
Figure 4. (a) Difference gradient vector $\mathbf{g}^{01}$ and nonadiabatic coupling vector $\mathbf{h}^{01}$ for the twisted conical intersection optimized at the MR-CISD/SA-3-CAS(2,2)/aug′-cc-pVTZ level. (b) Linearized adiabatic energies for the twisted conical intersection in the g−h (x−y) space. Energy in eV and x and y in Å.
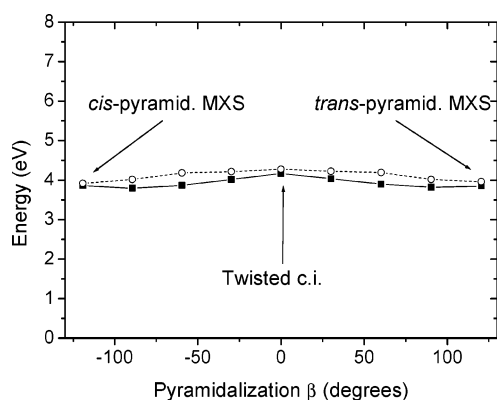

Figure 5. S_1 and S_2 potential energy curves for the pyramidalization of the CH_2 group.

ethylene connecting the pyramidalized MXS to the H-migration conical intersection.[59,63] In fluoroethylene we are observing the same feature, only displaced to small H-migration angles. An important distinction between the pyramidalized MXSs in ethylene and fluoroethylene is that in the former there is a strong degree of migration in one of the H atoms of the pyramidalized group, which results in a highly asymmetric structure. In fluoroethylene, this asymmetry is not observed in any of the pyramidalized MXSs and, therefore, the structures belong to the C_s point group.

In ethylene, Ben-Nun and Martinez[10] have shown that an ethylidene (CH_3CH) conical intersection exists. Later on,

Toniolo et al.[64] located the symmetry-required C_{3v}-ethylidene conical intersection. Recently, we have generalized these results[59] by showing that part of the S_0/S_1 crossing seam of ethylene lies also in the ethylidene region and that these two conical intersections belong to this seam. In other previous work,[10] we have shown that in the photochemical process, this region of the seam is responsible from 10% to 30% of the $S_1 \rightarrow S_0$ conversions. In analogy to ethylene, we have located three points of intersection in the CH_3CF and CH_2FCH regions of the configuration space of fluoroethylene. The structures of the CH_3CF and CH_2FCH MXSs are shown in Figure 3 and the energies of both and also of the C_{3v} conical intersection (linear CCF axis) are given in Table 4.

The C_{3v} conical intersection was studied previously by Bacskay.[28] In this work it was pointed out that this conical intersection could be responsible for the internal conversion during the $CH_3CF \rightarrow CH_2CHF$ isomerization process. A barrier of 0.89 eV has been computed between the system initially prepared in the S_1 state (vertical excitation) of the CH_3CF isomer and the C_{3v} conical intersection. We note, however, that the true MXS, as mentioned above, is distorted from the C_{3v} intersection. Our best result for this barrier is 0.27 eV, significantly reduced in comparison to the 0.89 eV presented by Bacskay. Therefore this MXS should be considered a better candidate for the main S_1−S_0 funnel in this region of the configuration space than the C_{3v} conical intersection.

For ethylene, the same seam connects the H-migration conical intersection and the intersection in the ethylidene region of the configuration space.[59] We expect that the same will occur for fluoroethylene even though we did not search for this path. One indication that this connection should exist in the present case also is the H-migration conical intersection that we have found for large H-migration angles (Figure 3 and Table 4). Probably, this conical intersection does not correspond to a minimum but to a saddle point on the crossing seam in analogy to the ethylene case.[63] We did not follow this question in more detail here since the energy of this intersection is relatively high.

It is well-known (see, e.g., Atchity et al.[3] and Jasper and Truhlar[65]) that the topography of the region around a conical intersection has an influence on the dynamics of the system. For instance, depending on the inclination or on the symmetry of the double cone, there will be a different probability of returning to the upper state. Following Yarkony,[2,66] these topographic features can be described in terms of a set of four parameters:

$$\sigma_x = \frac{\mathbf{s}^{01} \cdot \hat{\mathbf{x}}}{d_{gh}} \tag{1a}$$

$$\sigma_y = \frac{\mathbf{s}^{01} \cdot \hat{\mathbf{y}}}{d_{gh}} \tag{1b}$$

$$\Delta_{gh} = \frac{(g^2 - h^2)}{d_{gh}^2} \tag{1c}$$

$$d_{gh} = (g^2 + h^2)^{1/2} \tag{1d}$$

where $\mathbf{s}^{01}$ is the gradient sum vector and $(\hat{\mathbf{x}}, \hat{\mathbf{y}})$ are unit vectors based on Schmidt-orthogonalized vectors $\mathbf{g}$ (energy gradient difference) and $\mathbf{h}$ (nonadiabatic coupling vector):

$$\hat{\mathbf{x}} = \mathbf{g}^{01}/g, \qquad g = ||\mathbf{g}^{01}|| \tag{2}$$

$$\hat{\mathbf{y}} = \mathbf{h}^{01}/h, \qquad h = ||\mathbf{h}^{01}|| \tag{3}$$

Excited-State Energy Surfaces of Fluoroethylene

J. Phys. Chem. A, Vol. 109, No. 23, 2005 **5173**

TABLE 5: Topographic Parameters for the S_0/S_1 Conical Intersections[a]

structure[b]	parameters			
	σ_x	σ_y	Δ_{gh}	d_{gh} (eV/Å)
cis pyramidal	−0.377	−0.408	−0.01	5.46
trans pyramidal	−0.700	0.000	0.18	6.04
twisted CI	−0.925	0.006	0.08	6.76
CH_2FCH MXS	−4.610	1.232	0.22	0.82
CH_3CF MXS	3.148	−0.051	0.30	2.16
H-migration	0.327	−0.006	−0.50	7.15

[a] $\sigma_x = \sigma_y = \Delta_{gh} = 0$ corresponds to a symmetrical and vertical (peaked) conical intersection. [b] ci = conical intersection. MXS = minima on the crossing seam.

In terms of displacements x and y along $\hat{\mathbf{x}}$ and $\hat{\mathbf{y}}$, respectively, the linear approximation for the adiabatic energies of S_0 and S_1 is given by:[66]

$$E = d_{gh}\left[\sigma_x x + \sigma_y y \pm \left(\frac{1}{2}(x^2 + y^2) + \frac{\Delta_{gh}}{2}(x^2 - y^2)\right)^{1/2}\right] \quad (4)$$

From eq 4 we see that σ_i controls the tilt of the cone away from the vertical direction, Δ_{gh} determines the deviation from cylindrical symmetry, and d_{gh} controls the pitch of the cone.

Table 5 presents σ_x, σ_y, Δ_{gh}, and d_{gh} for the MXSs of fluoroethylene. All conical intersections contain some degree of asymmetry and tilt, as one can see, for example, in Figure 4b for the twisted conical intersection. In the present coordinate system, the tilt is in the direction of x for most of the conical intersections and only the cis-pyramidalized and CH_2FHC MXSs present some appreciable tilt in the direction of y. The asymmetry parameter Δ_{gh} has small positive values for most of the intersections, which means that the cones are slightly elongated in the direction y. The cis-pyramidalized structure has practically cylindrical symmetry and the H-migration conical intersection is strongly elongated in the x direction. There is a very clear distinction between the pitches of these conical intersections: while the twisted, the cis- and trans-pyramidalized and the H-migration conical intersections have similar d_{gh} values, the CH_2FCH and the CH_3CF MXSs show much smaller ones. For these two latter MXSs, the small d_{gh} and large σ_x values make them particularly sloped and therefore inefficient for the $S_1 \rightarrow S_0$ conversion. This situation is quite similar to that found in ethylene, for which the $S_1 \rightarrow S_0$ conversion occurs more efficiently at the peaked pyramidalized MXS than at the sloped ethylidene one.[10,11]

3.d. The Hula-Twist Process. In monoolefins and asymmetrical (polar) conjugated polyenes, after photoexcitation into the $\pi\pi^*$ state, the system is stabilized by a torsion around the CC bond in which the double bond is broken. Therefore, this torsional motion or one-bond-flip process (OBF) should be the main process driving the cis−trans isomerization of these classes of systems in the gas phase.[7] An alternative process that can also allow for cis−trans isomerization is the Hula-Twist (HT).[67,68] Different from the OBF process, in the HT process the variation of the volume is relatively small,[69] and for this reason it is used to explain cis−trans photoisomerization in environment-restricted systems.[70]

Since volume restrictions are not imposed in the present case of fluoroethylene, the cis−trans isomerization in fluoroethylene is expected to occur mainly through an OBF mechanism. Nevertheless, fluoroethylene is one of the smallest systems for which HT is structurally possible. Because of the general importance of HT we want to give a short discussion on it here also. In Figure 6 a possible realization of the HT motion as
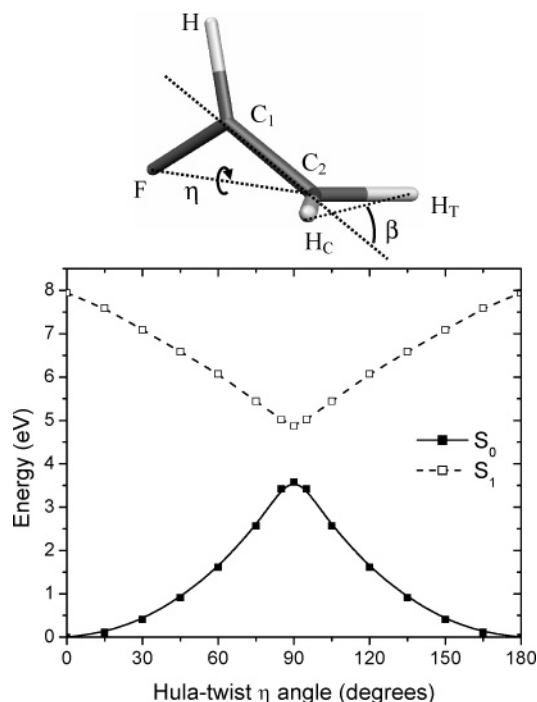

Figure 6. Potential energy curves for the Hula-Twist (HT) process. η is the HT angle and β is the pyramidalization angle.

presented in ref 67 is given in terms of internal coordinates. Our definition consists of the torsion of the atoms H and H_C around an axis defined by the nonbonded atoms F and C_2, allowing pyramidalization of the $C_2H_CH_T$ group also. Moreover, C_1 is always kept in the C_2FH plane and C_2 is always located in the H_CH_TF plane. Both criteria are achieved by freezing the out-of-plane angles[71] C_1C_2FH and $C_2H_CH_TF$ at the planar ground-state values. The Hula-Twist angle η itself is defined as the dihedral angle H_CC_2FH. For each value of η, all other internal coordinates (excepting the two frozen out-of-plane angles) were optimized for the S_1 state at the MR-CISD/SA-3-CAS(2,2)/aug-cc-pVDZ level of theory.

Thus, as for the OBF (Figure 1), HT stabilizes the S_1 state, and in this state the cis−trans isomerization can occur without barrier. However, while in OBF we have observed a very small gap between S_0 and S_1 (see Subsection 3.a), in HT the minimum gap is 1.3 eV occurring at the H_CC_2FH dihedral angle of 90°. The 90° structure shows a slight pyramidalization of the twisted-orthogonal structure, which means that the HT can easily result in structures near the S_0/S_1 crossing seam that connects the twisted conical intersection to the pyramidalized one. As we discuss in Subsection 3.d, this is the same branch of seam that is reached by the torsion (OBF) motion.

For larger systems with large momentum of inertia associated with the rotating groups in OBF, HT may become crucial not only as a pathway to the cis−trans pyramidalization, but also as a way of reaching the pyramidalized S_0/S_1 crossing seam. This can be the case, for example, for stilbene for which Quenneville and Martínez[72] have shown the existence of a MXS at the pyramidalized CHR group (R is the C_6H_5 ring). For a more complete discussion about the MXSs in stilbene and the role of the HT process in this system see refs 73 and 74.

3.e. Photodynamics of Fluoroethylene. As discussed in the Introduction, one important topic in the research of the halo-ethylenes is the determination of the elementary processes resulting in hydrogen halide and H_2 elimination. Since most of experiments have been performed with excitation energies close to the $\pi\pi^*$ absorption band (see, e.g., refs 14, 16, 17, and 23)

and the relaxation to the ground state seems to be a main process leading to several dissociation channels,[17] it is a central task to describe the just-mentioned relaxation processes and their relevance for the elimination processes.

For the dynamics through the S_0/S_1 seam we can deduct the following mechanism for the initial stages of the temporal evolution of fluoroethylene, and probably also of the other haloethylenes, in comparison to the photochemistry of ethylene.[75,76] After photoexcitation to the V ($\pi\pi^*$) state, the system can quickly evolve through torsional motions (OBF) that have the general effect of strongly reducing its potential energy. After just a few tens of femtoseconds, the system reaches the region of the twisted crossing seam, in which it can return to the ground state. With the large excess of internal energy, the fragmentation processes, including the HF elimination, might be completed in a time scale of a few hundreds of femtoseconds. On the other hand, in ethylene, the H_2 elimination is expected to occur in times from 800 to 3800 fs, depending on the photoexcitation energy.[77]

After a nonadiabatic transition, the acquired-vibrational energy is concentrated in a small number of vibrational modes that define the conical intersection.[78] For the twisted conical intersection, we can see from Figure 4a that these modes are composed mainly of torsion, CC stretching, and H-migration. The two latter modes can promote the formation of the CH_2-FCH isomer, a fact that has not been considered in the analysis of the experimental data up to now. Since two of the three HF exit channels in the CH_2FCH isomer correspond to three-center elimination, the presence of this isomer in the ground-state population should increase the probability of this type of elimination over the four-center one.

4. Conclusions

MR-CISD calculations have been performed for conical intersections and stationary structures on the fluoroethylene ground- and excited-state energy surfaces with recently developed methods for the computation of analytic gradients and nonadiabatic coupling terms.

For the planar ground-state geometry, the vertical spectrum (including 3s and 3p Rydberg states) was calculated with the MR-CISD and RI-CC2 methods. We observe a general good agreement with the experimental results with some need for further improvements in the notoriously difficult $\pi\pi^*$ excitation.

From the planar ground-state geometry, a rigid torsion around the CC bond strongly reduces the energy gap between the S_0 and S_1 states. Furthermore, the optimization process shows that there is a conical intersection very close to the twisted structure and two others in pyramidalized structures. We have also shown that all three intersections are connected by the same seam and that the Hula-Twist process is an alternative way to reach the crossing seam. Other conical intersections were located close to the CH_3CF and CH_2FCH and H-migration structures and to the CH_3CF C_{3v} structure.

On the basis of topological features of these MXSs, we have argued that the S_1-S_0 conversion after photoexcitation at the planar global minimum should take place mainly at the twisted conical intersection. This process is markedly different from that in ethylene, in which a strong pyramidalization is needed before the conversion takes place. We have pointed out that the occurrence of the nonadiabatic transition through the twisted conical intersection may imply that the CH_2FCH isomer is significantly populated and therefore it should be taken into account in the experimental and theoretical analysis of the three- and four-center HF elimination.

References and Notes

(1) v. Neumann, J.; Wigner, E. *Phys. Z.* **1929**, *30*, 467.
(2) Yarkony, D. R. In *Conical Intersections*; Advanced Series in Physical Chemistry 15; Domcke, W., Yarkony, D. R., Köppel, H., Eds.; World Scientific: Singapore, 2004; p 129.
(3) Atchity, G. J.; Xantheas, S. S.; Ruedenberg, K. *J. Chem. Phys.* **1991**, *95*, 1862.
(4) Bearpark, M. J.; Robb, M. A.; Schlegel, H. B. *Chem. Phys. Lett.* **1994**, *223*, 269.
(5) Lischka, H.; Dallos, M.; Szalay, P. G.; Yarkony, D. R.; Shepard, R. *J. Chem. Phys.* **2004**, *120*, 7322.
(6) Molnar, F.; Ben-Nun, M.; Martínez, T. J.; Schulten, K. *J. Mol. Struct.* (*THEOCHEM*) **2000**, *506*, 169.
(7) Ruiz, D. S.; Cembran, A.; Garavelli, M.; Olivucci, M.; Fuss, W. *Photochem. Photobiol.* **2002**, *76*, 622.
(8) Migani, A.; Olivucci, M. In *Conical Intersections*; Advanced Series in Physical Chemistry 15; Domcke, W., Yarkony, D. R., Köppel, H., Eds.; World Scientific: Singapore, 2004; p 271.
(9) Robb, M. A.; Garavelli, M.; Olivucci, M.; Bernardi, F. In *Reviews in Computational Chemistry*; Lipkowitz, K. B., Boyd, D. B., Eds.; Wiley-VCH Publishers: New York, 2000; Vol. 15, p 87.
(10) Ben-Nun, M.; Martínez, T. J. *J. Chem. Phys.* **2000**, *259*, 237.
(11) Barbatti, M.; Ruckenbauer, M.; Lischka, H. *J. Chem. Phys.* **2005**, *122*, 174307.
(12) Pitonak, M.; Lischka, H. *Mol. Phys.* **2005**, *103*, 855.
(13) Lischka, H.; Aquino, A. J. A.; Barbatti, M.; Solimannejad, M. In *Lecture Notes in Computer Science*; Gervasi, O., et al., Eds.; Springer-Verlag: Berlin, 2005; Vol. 3480, p 1004.
(14) Berry, M. J.; Pimentel, G. C. *J. Chem. Phys.* **1969**, *51*, 2274.
(15) Kato, S.; Morokuma, K. *J. Chem. Phys.* **1981**, *74*, 6285.
(16) Lin, S.-R.; Lin, S.-C.; Lee, Y.-C.; Chou, Y.-C.; Chen, I.-C.; Lee, Y.-P. *J. Chem. Phys.* **2001**, *114*, 160.
(17) Lin, S.-R.; Lin, S.-C.; Lee, Y.-C.; Chou, Y.-C.; Chen, I.-C.; Lee, Y.-P. *J. Chem. Phys.* **2001**, *114*, 7396.
(18) Güthe, F.; Locht, R.; Leyh, B.; Baumgärtel, H.; Weitzel, K.-M. *J. Phys. Chem. A* **1999**, *103*, 8404.
(19) Güthe, F.; Locht, R.; Baumgärtel, H.; Weitzel, K.-M. *J. Phys. Chem. A* **2001**, *105*, 7508.
(20) Yoon, S. H.; Choe, J. C.; Kim, M. S. *Int. J. Mass Spectrom.* **2003**, *227*, 21.
(21) Kunsági-Máté, S.; Végh, E.; Nagy, G.; Kollár, L. *Chem. Phys. Lett.* **2004**, *388*, 84.
(22) Martínez-Núñez, E.; Vásquez, S. A. *J. Chem. Phys.* **2004**, *121*, 5179.
(23) Sato, K.; Tsunashima, S.; Takayanagi, T.; Fijisawa, G.; Yokoyama, A. *Chem. Phys. Lett.* **1995**, *242*, 401.
(24) Smith, B. J.; Coffey, D., Jr.; Radom, L. *J. Chem. Phys.* **1992**, *97*, 6113.
(25) Martínez-Núñez, E.; Vásquez, S. A. *Struct. Chem.* **2001**, *12*, 95.
(26) Ljubić, I.; Sabljić, A. *J. Phys. Chem. A* **2002**, *106*, 4745.
(27) Li, L.-C.; Deng, P.; Xu, M.-H.; Wong, N.-B. *Int. J. Quantum Chem.* **2004**, *98*, 309.
(28) Bacskay, G. B. *Mol. Phys.* **2003**, *101*, 1955.
(29) Bunge, A. *J. Chem. Phys.* **1970**, *53*, 20.
(30) Dunning, T. H., Jr. *J. Chem. Phys.* **1989**, *90*, 1007.
(31) Kendall, R. A.; Dunning, T. H., Jr.; Harrison, R. J. *J. Chem. Phys.* **1992**, *96*, 6769.
(32) Langhoff, S. R.; Davidson, E. R. *Int. J. Quantum Chem.* **1974**, *8*, 61.
(33) Bruna, P. J.; Peyerimhoff, S. D.; Buenker; R. J. *Chem. Phys. Lett.* **1981**, *72*, 278.
(34) Woon, D. E.; Dunning, T. H., Jr. *J. Chem. Phys.* **1994**, *100*, 2975.
(35) van Mourik, T.; Wilson, A. K.; Dunning, T. H., Jr. *Mol. Phys.* **1999**, *96*, 529.
(36) Müller, T.; Dallos, M.; Lischka, H. *J. Chem. Phys.* **1999**, *110*, 7176.
(37) Dallos, M.; Lischka, H. *Theor. Chem. Acc.* **2004**, *112*, 16.
(38) Shepard, R. *Adv. Chem. Phys.* **1987**, *69*, 63.

Excited-State Energy Surfaces of Fluoroethylene

J. Phys. Chem. A, Vol. 109, No. 23, 2005 **5175**

(39) Bobrowicz, F. W.; Goddard, W. A., III In *Methods of Electronic Structure Theory*; Schaefer, H. F., III, Ed.; Plenum: New York, 1977; p 79.

(40) Christiansen, O.; Koch, H.; Jørgensen, P. *Chem. Phys. Lett.* **1995**, *243*, 409.

(41) Hättig, C.; Köhn, A. *J. Chem. Phys.* **2002**, *117*, 6939.

(42) Hättig, C. *J. Chem. Phys.* **2003**, *118*, 7751.

(43) Köhn, A.; Hättig, C. *J. Chem. Phys.* **2003**, *119*, 5021.

(44) Shepard, R. *Int. J. Quantum Chem.* **1987**, *31*, 33.

(45) Shepard, R.; Lischka, H.; Szalay, P. G.; Kovar, T.; Ernzerhof, M. *J. Chem. Phys.* **1992**, *96*, 2085.

(46) Shepard, R. In *Modern Electronic Structure Theory Part I*; Yarkony, D. R., Ed.; World Scientific: Singapore, 1995; p 345.

(47) Lischka, H.; Dallos, M.; Shepard, R. *Mol. Phys.* **2002**, *100*, 1647.

(48) Dallos, M.; Lischka, H.; Shepard, R.; Yarkony, D. R.; Szalay, P. G. *J. Chem. Phys.* **2004**, *120*, 7330.

(49) Császár, P.; Pulay, P. *J. Mol. Struct.* **1984**, *114*, 31.

(50) Fogarasi, G.; Zhou, X.; Taylor, P. W.; Pulay, P. *J. Am. Chem. Soc.* **1992**, *114*, 8191.

(51) Lischka, H.; Shepard, R.; Brown, F. B.; Shavitt, I. *Int. J. Quantum Chem.* **1981**, *15*, 91.

(52) Shepard, R.; Shavitt, I.; Pitzer, R. M.; Comeau, D. C.; Pepper, M.; Lischka, H.; Szalay, P. G.; Ahlrichs, R.; Brown, F. B.; Zhao, J. *Int. J. Quantum Chem., Quantum Chem. Symp.* **1988**, *22*, 149.

(53) Lischka, H.; Shepard, R.; Pitzer, R. M.; Shavitt, I.; Dallos, M.; Müller, Th.; Szalay, P. G.; Seth, M.; Kedziora, G. S.; Yabushita, S.; Zhang, Z. *Phys. Chem. Chem. Phys.* **2001**, *3*, 664.

(54) Lischka, H.; Shepard, R.; Shavitt, I.; Pitzer, R. M.; Dallos, M.; Müller, Th.; Szalay, P. G.; Brown, F. B.; Ahlrichs, R.; Böhm, H. J.; Chang, A.; Comeau, D. C.; Gdanitz, R.; Dachsel, H.; Ehrhardt, C.; Ernzerhof, M.; Höchtl, P.; Irle, S.; Kedziora, G.; Kovar, T.; Parasuk, V.; Pepper, M. J. M.; Scharf, P.; Schiffer, H.; Schindler, M.; Schüler, M.; Seth, M.; Stahlberg, E. A.; Zhao, J.-G.; Yabushita, S.; Zhang, Z. *COLUMBUS*, an ab initio electronic structure program, release 5.9, 2004.

(55) Helgaker, T.; Jensen, H. J. Aa.; Jørgensen, P.; Olsen, J.; Ruud, K.; Ågren, H.; Andersen, T.; Bak, K. L.; Bakken, V.; Christiansen, O.; Dahle, P.; Dalskov, E. K.; Enevoldsen, T.; Heiberg, H.; Hettema, H.; Jonsson, D.; Kirpekar, S.; Kobayashi, R.; Koch, H.; Mikkelsen, K. V.; Norman, P.; Packer, M. J.; Saue, T.; Taylor, P. R.; Vahtras, O. *DALTON*, an ab initio electronic structure program, Release 1.0, 1997.

(56) Ahlrichs, R.; Bär, M.; Häser, M.; Horn, H.; Kölmel, C. *Chem. Phys. Lett.* **1989**, *162*, 165.

(57) Bélanger, G.; Sandorfy, C. *J. Phys. Chem. A* **1971**, *55*, 2055.

(58) Petrongolo, C.; Buenker, R. J.; Peyerimhoff, S. D. *J. Chem. Phys.* **1982**, *76*, 3655.

(59) Barbatti, M.; Paier, J.; Lischka, H. *J. Chem. Phys.* **2004**, *121*, 11614.

(60) Krawczyk, R. P.; Viel, A.; Manthe, U.; Domcke, W. *J. Chem. Phys.* **2003**, *119*, 1397.

(61) Bonačić-Koutecký, V.; Koutecký, J.; Michl, J. *Angew. Chem.*, *Int. Ed.* **1987**, *26*, 170.

(62) Michl, J.; Bonačić-Koutecký, V. *Electronic Aspects of Organic Photochemistry*; Wiley: New York, 1990.

(63) Laino, T.; Passerone, D. *Chem. Phys. Lett.* **2004**, *389*, 1.

(64) Toniolo, A.; Ben-Nun, M.; Martínez, T. J. *J. Phys. Chem. A* **2002**, *106*, 4679.

(65) Jasper, A. W.; Truhlar, D. G. *J. Chem. Phys.* **2005**, *122*, 044101.

(66) Yarkony, D. R. *J. Chem. Phys.* **2001**, *114*, 2601.

(67) Liu, R. S. H.; Asato, A. E. *Proc. Natl. Acad. Sci. U.S.A.* **1985**, *82*, 259.

(68) Muller, A. M.; Lochbrunner, S.; Schmid, W. E.; Fuss, W. *Angew. Chem.*, *Int. Ed.* **1998**, *37*, 505.

(69) Liu, R. S. H.; Hammond, G. S. *Chem. Eur. J.* **2001**, *7*, 4536.

(70) Wald, G. *Science* **1968**, *162*, 230.

(71) Wilson, E. B.; Decius, J. C.; Cross, P. C. *Molecular vibrations: the theory of infrared and Raman vibrational spectra*; McGraw-Hill: New York, 1955; p 58.

(72) Quenneville, J.; Martínez, T. J. *J. Phys. Chem. A* **2003**, *107*, 829.

(73) Bearpark, M. J.; Bernardi, F.; Clifford, S.; Olivucci, M.; Robb, M. A.; Vreven T. *J. Phys. Chem. A* **1997**, *101*, 3841.

(74) Fuss, W.; Kosmidis, C.; Schmid, W. E.; Trushin, S. A. *Angew. Chem.*, *Int. Ed.* **2004**, *43*, 4178.

(75) Ben-Nun, M.; Quenneville, J.; Martínez, T. J. *J. Phys. Chem. A* **2000**, *104*, 5161.

(76) Barbatti, M.; Granucci, G.; Persico, M.; Lischka, H. *Chem. Phys. Lett.* **2005**, *401*, 276.

(77) Peña-Gallego, A.; Martínez-Núñez, E.; Vázquez, S. A. *Chem. Phys. Lett.* **2002**, *353*, 418.

(78) Domcke, W. In *Conical Intersections*; Advanced Series in Physical Chemistry 15; Domcke, W., Yarkony, D. R., Köppel, H., Eds.; World Scientific: Singapore, 2004; p 395.